

STUDIES OF SMALL H II REGIONS. I. INFRARED PHOTOMETRY OF SHARPLESS 138, 152, AND 270

JAY A. FROGEL* AND S. ERIC PERSSON*

Harvard College Observatory

Received 1972 April 20; revised 1972 July 20

ABSTRACT

Multiperture photometric observations from 1.6 to 3.5 μ of three small H II regions, Sharpless 138, 152, and 270, are presented. These three objects are shown to be representative of a distinct class of H II regions. The spatial and spectral distributions of the flux are similar for the three objects: surface brightnesses and apparent color temperatures generally decrease with increasing distance from the infrared centers. The integrated colors are: [1.6 μ] - [2.2 μ] \sim 1.0 mag, [2.2 μ] - [3.5 μ] \sim 2.5 mag, similar to those of NGC 7027.

A plausible interpretation of the observations is that the infrared flux arises from a mixture of recombination emission and thermal radiation from dust particles. The 3.5- μ limb-brightening observed in Sh 152 could indicate the presence of a dust shell with an inner radius of \sim 16".

I. INTRODUCTION

Infrared observations of H II regions have in the past generally been restricted to the Orion Nebula, M8, and M17 (summarized by Neugebauer, Becklin, and Hyland 1971). The catalog of Sharpless (1959), however, lists many small (< 10 arc min) H II regions which are well suited to study with a telescope of small or moderate size. Previous observations of some of the objects in Sharpless's catalog have consisted of radio-continuum flux measurements (Churchwell and Felli 1970; Terzian 1970; Felli and Churchwell 1972) and a radial-velocity survey by Miller (1968). This paper is a preliminary report of infrared photometric observations that are part of an infrared, optical, and radio study of the Sharpless regions currently under way at Harvard.

II. OBSERVATIONS

Broad-band infrared photometric observations at 1.6, 2.2, and 3.5 μ^1 of the objects Sh 138, 152, and 270 were made with a PbS detecting system that has cooled filters and focal-plane apertures. These particular objects were selected on the basis of one or more of the following criteria: small ($< 2'$) optical size; extreme redness as evidenced by comparing the red and blue *Palomar Sky Survey* prints; internal obscuration visible on the *Sky Survey* prints (see fig. 1 [pl. 8]). The measured magnitudes and fluxes are given in table 1. Most of the observations were made with the 60-inch (152-cm) Tillinghast reflector of Mount Hopkins Observatory; they were corrected for flux in the reference beam, which is separated by 69" from the signal beam. This correction was negligible for the two smaller objects, but for Sh 152 it amounted to typically 10 percent at 1.6 μ , 10 percent at 2.2 μ , and 20 percent at 3.5 μ (correction/total). The measurements with apertures of 57", 85", and 116" were made on the f/7.5, 36-inch (91-cm) telescope of Kitt Peak National Observatory (KPNO), under marginal observing conditions.

* Visiting Astronomer, 1972, Kitt Peak National Observatory, which is operated by the Association of Universities for Research in Astronomy, Inc., under contract with the National Science Foundation.

¹ Hereinafter the magnitude at a particular wavelength λ will be denoted by [$\lambda\mu$].

PLATE 8

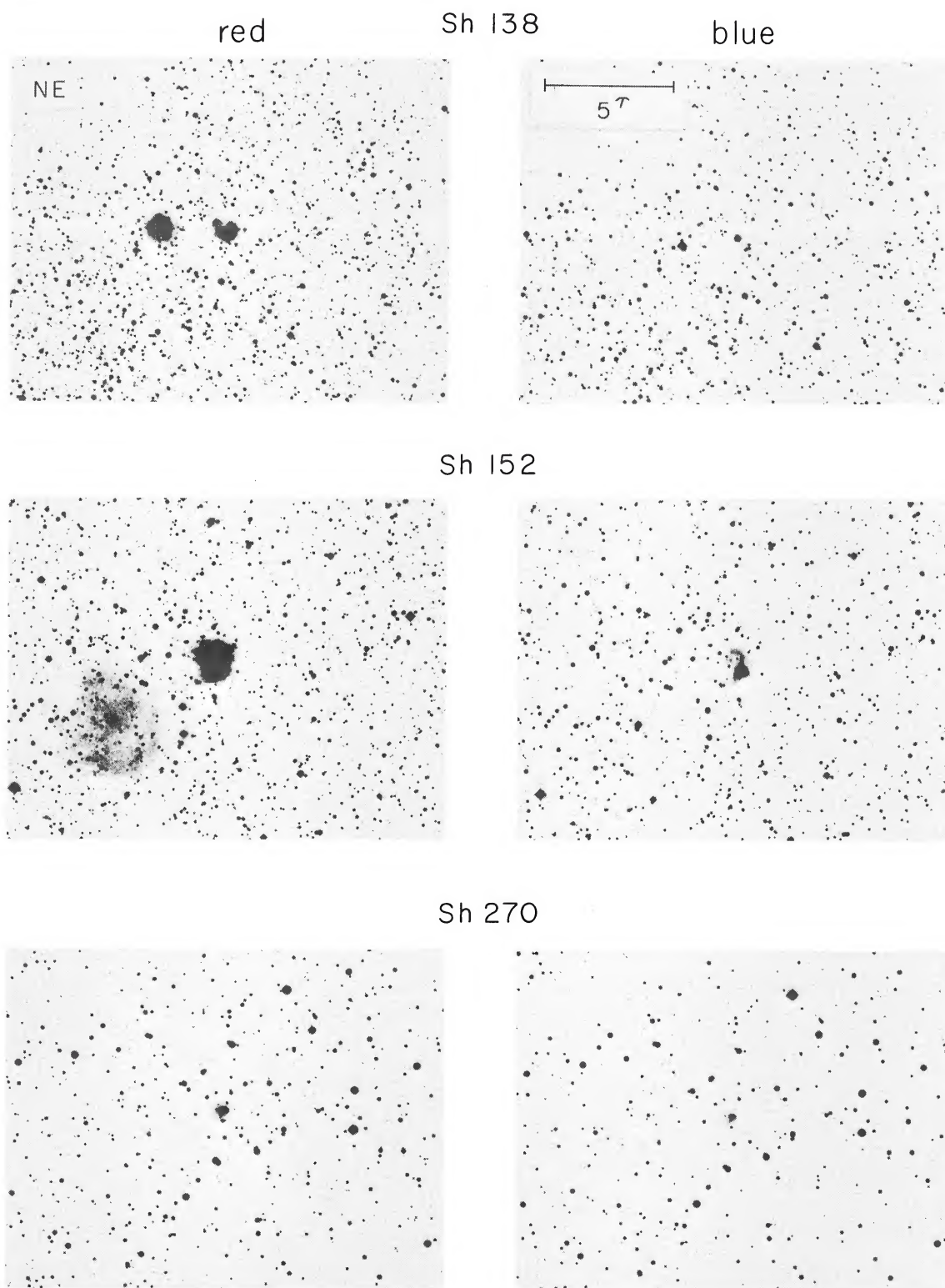


FIG. 1.—Red and blue finding charts of three H II regions. In all cases north is up and east is to the left. The indicated scale is the same for each chart. These photographs were reproduced from the *Palomar Sky Survey* prints.

FROGEL AND PERSSON (*see* page 667)

TABLE 1
 INFRARED PHOTOMETRY OF H II REGIONS
 Magnitude ($\pm 1 \sigma$)
 $F_{\nu}(10^{-26} \text{W m}^{-2} \text{Hz}^{-1})$

Aperture Diameter (Arc Sec)	Sh 138			Sh 152			Sh 270		
	1.65 μ	2.2 μ	3.5 μ	1.65 μ	2.2 μ	3.5 μ	1.65 μ	2.2 μ	3.5 μ
15.....	9.29(0.10) 0.20	8.25(0.06) 0.32	6.88(0.06) 0.53	9.36(0.10) 0.19	9.02(0.06) 0.16	8.27(0.17) 0.14	11.25(0.33) 0.033	10.23(0.14) 0.052	8.28(0.17) 0.14
22.....	8.84(0.08) 0.30	7.91(0.07) 0.44	6.28(0.08) 0.91	9.16(0.09) 0.22	8.57(0.07) 0.24	7.70(0.13) 0.25	10.91(0.14) 0.045	9.58(0.06) 0.095	7.51(0.14) 0.29
27.....	8.85(0.10) 0.30	7.84(0.05) 0.48	5.97(0.09) 1.21	9.00(0.07) 0.26	8.38(0.05) 0.29	7.45(0.21) 0.31	10.44(0.17) 0.071	9.24(0.08) 0.13	7.30(0.13) 0.36
40.....	8.62(0.07) 0.38	7.50(0.07) 0.64	5.60(0.08) 1.70	8.60(0.07) 0.38	7.92(0.07) 0.44	6.07(0.13) 1.10	9.92(0.11) 0.11	8.91(0.07) 0.18	6.78(0.45) 0.58
55.....	8.53(0.09) 0.41	7.34(0.06) 0.74	5.23(0.16) 2.38	8.40(0.10) 0.46	7.60(0.07) 0.59	5.60(0.15) 1.70	9.88(0.12) 0.12	9.02(0.10) 0.16	6.36(0.24) 0.83
57.....	8.26(0.11) 0.52	7.44(0.06) 0.69	5.13(0.28) 2.64		7.57(0.07) 0.60				
85.....	7.96(0.23) 0.68	7.29(0.07) 0.78	4.87(0.37) 2.32	8.10(0.10) 0.60	7.32(0.08) 0.76	4.92(0.25) 3.16			
116.....	8.11(0.12) 0.59	7.10(0.06) 0.93		8.17(0.11) 0.56	7.22(0.07) 0.83	4.77(0.21) 3.63			

The regions were scanned with a small aperture at 2.2μ , and only one well-defined emission peak was found in each. In particular, no point sources with $[2.2 \mu] < 10$ were found in any of the regions. All measurements were made with apertures centered on the positions of maximum flux. The efficacy of the centering procedure was verified by repeating some of the measurements on different nights. The observational method employed necessitates the assumption of the spherical symmetry of the objects. However, departures from spherical symmetry will not systematically affect the results described below.

III. RESULTS

The results of this investigation are presented graphically in figures 2 and 3. Figure 2 displays the infrared energy spectra of the H II regions for each aperture used. It is evident that in these objects the infrared colors depend strongly on aperture and that except for the smaller-aperture measurements of Sh 152, the spectra cannot be accounted for by atomic recombination emission at any temperature. Figure 3 gives the flux at each wavelength as a function of aperture diameter. For a source of constant surface brightness the flux will vary as shown by the dashed line. With the exception of Sh 152 at 3.5μ , the flux at each wavelength increases more slowly than this with aperture. In the absence of point sources this means that the surface brightnesses of the H II regions generally decrease with increasing distance from the center. Finally, the average surface brightnesses at a particular wavelength are quite similar for the three objects.

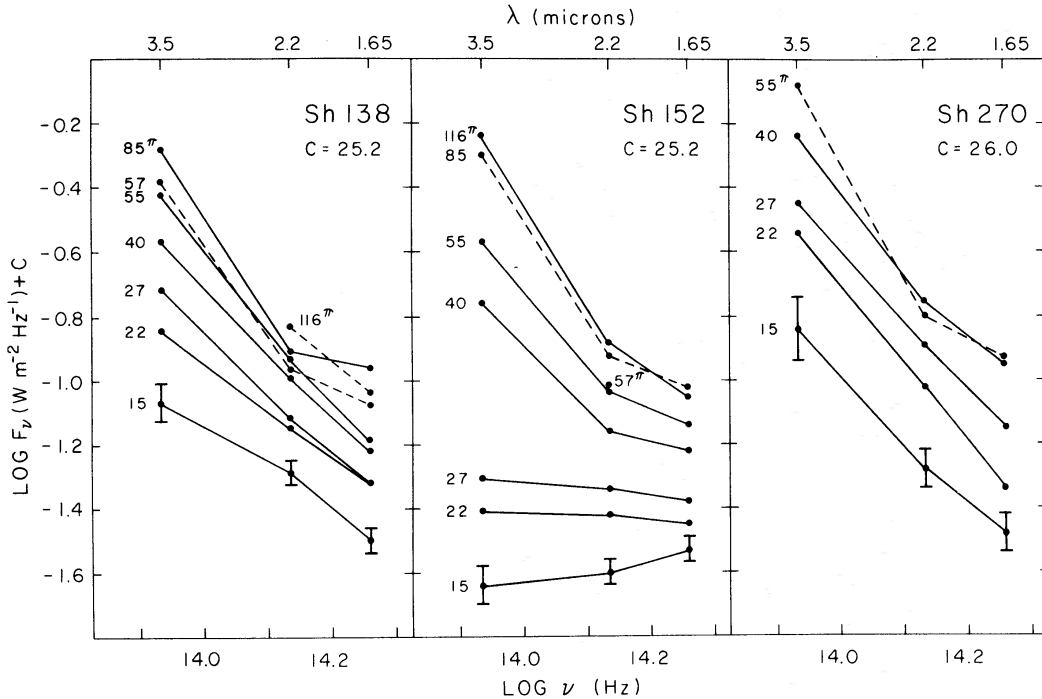


FIG. 2.—Log flux ($\text{W m}^{-2} \text{Hz}^{-1}$) versus $\log \nu$ (Hz) and λ (μ) for three H II regions. Each spectrum is labeled by the aperture diameter (arc sec) used.

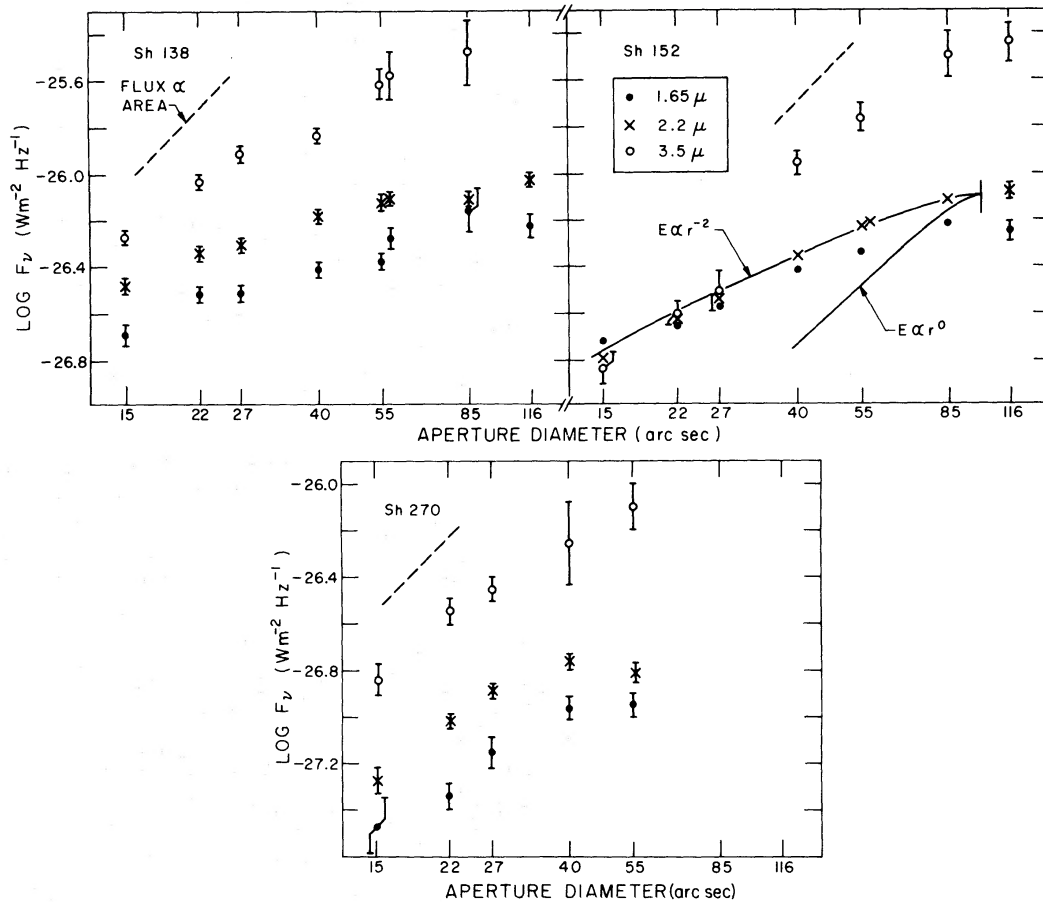


FIG. 3.—Log flux ($\text{W m}^{-2} \text{ Hz}^{-1}$) versus aperture diameter (arc sec) plotted logarithmically, for three H II regions. The dashed line in each plot shows the flux dependence for an object of constant surface brightness. The lines denoted $E \propto r^0$ and $E \propto r^{-2}$ are explained in the text.

IV. DESCRIPTION OF INDIVIDUAL OBJECTS

a) Sh 138

Nearly all of the 1.6–3.5 μ flux from this object comes from a region less than 1'.5 in diameter, comparable with the size of the overexposed image on the red *Palomar Sky Survey* print. There is a moderate increase in the [1.6 μ] – [2.2 μ] and [2.2 μ] – [3.5 μ] colors as the aperture size is increased. The colors found with the largest apertures are quite similar to those of the peculiar planetary nebula NGC 7027, viz., 1.1 and 2.4 mag, respectively (Willner, Becklin, and Visvanathan 1972). The surface brightness decreases smoothly with increasing distance from the infrared center, the decrease being most rapid at 1.6 and 2.2 μ and distinctly less so at 3.5 μ .

b) Sh 152

As in Sh 138, nearly all of the observed infrared flux from Sh 152 comes from a region corresponding in size with the dense image on the red *Palomar Sky Survey* print, and the colors measured with the largest apertures are similar to those of NGC 7027. Between 13" and 20" from the infrared center, the 3.5- μ flux increases sharply with increasing aperture, causing the color to be a strong function of aperture size.

Observations made on both sides of the discontinuity on two nights showed that this is not an observational artifact. Also, since the flux increases with aperture at the same rate on either side of the discontinuity, it is quite unlikely that the jump is due to a 3.5- μ point source.

c) Sh 270

Again the infrared and optical regions have comparable diameters, about 0'.8. There is only a weak dependence of color on aperture size, and the integrated colors are similar to those of NGC 7027. The dependence of flux on aperture diameter is quite smooth at all wavelengths.

A radio observation by Churchwell and Felli (1970) sets an upper limit of $0.5 \times 10^{-26} \text{ W m}^{-2} \text{ Hz}^{-1}$ to the 11-cm flux from Sh 270. This implies an upper limit of $0.12 \times 10^{-26} \text{ W m}^{-2} \text{ Hz}^{-1}$ at 3.5 μ , on the assumption that the 11-cm flux arises from optically thin free-free emission at a temperature of 10^4 ° K. The observed flux at 3.5 μ is greater than this by a factor of seven.

V. DISCUSSION

The observational results presented above may be used to determine some general properties of these H II regions. First, the relative infrared diameters are the same as the relative optical diameters of the objects. Also, since both the dependence of flux on aperture, and the integrated surface brightness at each wavelength are similar for the objects, it would appear that they are structurally similar. Color differences in the interior regions (see fig. 2) may then be accounted for by differences in angular size.

Second, the dependence of both the surface brightness and color on aperture implies that the objects cannot be optically thick at 1.65, 2.2, or 3.5 μ . This means that the observed dependence of the flux upon aperture (or equivalently, the surface brightness upon projected radius for a spherically symmetric object) can be used to derive the approximate dependence of the infrared emission coefficient E ($\text{W m}^{-3} \text{ Hz}^{-1}$) upon physical distance r from the center of each object. For example, in figure 3 (Sh 152) the dependences of flux on aperture are given for E varying as r^0 and r^{-2} in a spherically symmetric object whose diameter is 100 arc sec. (A proper comparison of these curves with the data at a particular wavelength depends upon knowledge of the size of the object at that wavelength.) An r^{-2} dependence is seen to fit the 2.2- μ data for Sh 152 quite well. It is difficult to fit the curve for $E \propto r^0$ to the 1.65- and 2.2- μ data for any value of the infrared diameter. Similar results are obtained for the other objects: the emission coefficients at all three wavelengths must decrease with increasing physical distance from the center.

Third, the integrated colors of the three regions are quite similar to one another and to those of NGC 7027. The color temperature, however, is significantly lower in the outer parts of each region than in the inner parts—a feature that is not observed in NGC 7027 (Kleinmann and Willner, unpublished). On the other hand, the objects are not as red as the compact H II region K3-50 (Neugebauer and Garmire 1970), for which $[2.2 \mu] - [3.5 \mu] \sim 3.5$. The infrared fluxes of both NGC 7027 and K3-50 have been interpreted as arising from thermal radiation by dust particles.

Fourth, the energy distributions observed in Sh 138 and 270, and in the outer regions of Sh 152, cannot be fitted by recombination emission alone at temperatures normally associated with H II regions. A reasonable interpretation of these energy spectra and the infrared excess observed in Sh 270 is that the flux arises from an as yet undetermined mixture of recombination emission and thermal radiation from dust, the latter dominating at 3.5 μ . The observed variation of infrared color with aperture then implies that the relative contributions of the dust and gas to the emission coefficient are functions of position within each object. In particular, with the exception of

the sharp increase in Sh 152 (see below), the general trend is for E at 3.5μ to decrease with increasing r at a rate slower than that for the shorter wavelengths. This difference can be interpreted as showing that the relative contribution to E of the dust emission increases with increasing r , in all cases. From the $[2.2 \mu] - [3.5 \mu]$ color an upper limit of 600°K can be set to the temperature of this dust near the outside of the objects.

In Sh 152 the $3.5\text{-}\mu$ flux increases by a factor of three in going from an aperture diameter of $27''$ to $40''$. This behavior could be interpreted as indicating the presence of a dust shell with an inner radius of $R \sim 16''$; for $R > 16''$, the dust emission dominates the recombination at 3.5μ . This obviates the need for a change in the physical temperature of the dust at this radius. The energy spectrum of the inner regions of Sh 152 is consistent with an unknown combination of recombination emission and starlight, the latter having $F_\nu \sim \nu^2$, which is characteristic of early-type stars. Thus Sh 152 and, by analogy, Sh 138 and 270, seem to display some of the properties postulated for the stellar cocoons discussed by Davidson and Harwit (1967), Davidson (1970), and Mathews (1965, 1967, 1969).

The common properties of the three regions suggest that excesses at 3.5μ will also be found in Sh 138 and 152 when radio data become available. Such excesses have been confirmed in other Sharpless regions for which both infrared and radio data are available (Frogel and Persson, in preparation).

VI. SUMMARY

The three H II regions discussed here, Sh 138, 152, and 270, are morphologically similar and are representative of a distinct class of H II regions characterized by some well-defined infrared properties: (1) uniform, red, integrated colors $[1.6 \mu] - [2.2 \mu] \sim 1.0 \text{ mag}$, $[2.2 \mu] - [3.5 \mu] \sim 2.5 \text{ mag}$; (2) apparent infrared color-temperatures that generally increase toward the centers of the regions; (3) infrared surface brightnesses that generally decrease with increasing angular distance from the center; (4) fluxes at 3.5μ that may be considerably in excess of that expected by extrapolating the thermal radio emission; (5) absence of infrared point sources having $[2.2 \mu] < 10$, corresponding to a flux of $7 \times 10^{-28} \text{ W m}^{-2} \text{ Hz}^{-1}$. Additionally, the *Palomar Sky Survey* prints provide evidence of considerable intrinsic obscuration.

We thank Drs. W. Liller, D. E. Kleinmann, and an anonymous referee for suggesting improvements in the manuscript. Mr. Rand Baldwin assisted with the KPNO observations and the data reduction. Mr. Bastiaan van't Sant provided valuable technical assistance. We thank the staff of KPNO for their help and hospitality.

REFERENCES

- Churchwell, E., and Felli, M. 1970, *A.J.*, **75**, 69.
 Davidson, K. 1970, *Ap. and Space Sci.*, **6**, 422.
 Davidson, K., and Harwit, M. 1967, *Ap. J.*, **148**, 443.
 Felli, M., and Churchwell, E. 1972, *Astr. and Ap. Suppl.* (in press).
 Mathews, W. G. 1965, *Ap. J.*, **142**, 1120.
 ———. 1967, *ibid.*, **147**, 965.
 ———. 1969, *ibid.*, **157**, 583.
 Miller, J. S. 1968, *Ap. J.*, **151**, 473.
 Neugebauer, G., Becklin, E., and Hyland, A. R. 1971, *Ann. Rev. Astr. and Ap.*, **9**, 67.
 Neugebauer, G., and Garmire, G. 1970, *Ap. J. (Letters)*, **161**, L91.
 Sharpless, S. 1959, *Ap. J. Suppl.*, **4**, 257.
 Terzian, Y. 1970, *A.J.*, **75**, 1155.
 Willner, S., Becklin, E., and Visvanathan, N. 1972, *Ap. J.* (in press).